

Research Article

Trajectory Control Algorithm of Flexible Joint Manipulator Based on Random Matrix and Screw Theory

Hao Guo , Dashuai Zhou, and Yao He

Department of Mechanical Manufacturing, School of Mines and Mechanical Engineering, Liupanshui Normal University, Liupanshui, Guizhou 553004, China

Correspondence should be addressed to Hao Guo; hg229@njit.edu

Received 25 April 2022; Revised 12 May 2022; Accepted 17 May 2022; Published 1 June 2022

Academic Editor: Ning Cao

Copyright © 2022 Hao Guo et al. This is an open access article distributed under the Creative Commons Attribution License, which permits unrestricted use, distribution, and reproduction in any medium, provided the original work is properly cited.

Flexible articulated manipulators are often used for the task of tracking reference trajectories in space and have attracted much attention. Aiming at the uncertainty of the robot system, based on random matrix and screw theory, this paper constructs a trajectory control model of a flexible joint manipulator. In order to reduce the steady-state tracking error, a random matrix variable structure control method is introduced into the model, and a nonlinear spinor-like random matrix function is designed to improve the traditional random matrix surface. In the simulation process, the dynamic model of the series robot is firstly obtained according to the screw and random matrix equation, and the dynamic characteristics are analyzed. Combined with dynamic surface control technology, a neural network controller is designed to solve the problem of dimensional explosion and ensure that the tracking error converges to a small neighborhood of zero. The experimental results show that by using the observation value to replace the unmeasurable state of the system, combining it with the random matrix network to identify the unknown dynamics of the system, and designing the random matrix network controller, the tracking control of the system can be realized, and the tracking error can be ensured to converge to a small neighborhood of zero. The control system has a better control effect than traditional PID, the peak time is shortened by 45.83%, the adjustment time is shortened by 46.91%, the maximum overshoot is reduced by 51.35%, and the steady-state error after filtering is only 0.049, which is reduced by 47.31%. Effective interference signal and measurement noise are suppressed, and the quantitative observation performance of the flexible joint manipulator system is improved.

1. Introduction

With the rapid development of modern industry, the application fields of robots are becoming more and more extensive. As the basic actuator of the robot, the robotic arm is often used to carry out tasks such as moving objects or tracking reference trajectories in space. Common manipulators include rigid manipulators and flexible manipulators. Flexible joint manipulators have significant advantages over traditional rigid manipulators in terms of response speed, control accuracy, and load-to-weight ratio, but they are highly nonlinear and strongly coupled, which brings great challenges to controller design [1–4]. Therefore, studying the random matrix network control and learning problems of flexible joint manipulators has

important theoretical significance and broad practical application prospects [5–7].

As the most commonly used robot in the industry, the early control method of the manipulator is mostly point-to-point control. This control scheme is suitable for scenarios with low precision requirements. With the increase in production technology, industrial manufacturing puts forward higher requirements for the control accuracy of the manipulator and, at the same time, requires the end of the manipulator to track the given reference trajectory motion [4, 8–10]. With the advent of the era of intelligent manufacturing, the tasks of the manipulator have become refined, and industrial production has put forward higher requirements for the accuracy of the manipulator [11–13]. At the same time, the

adaptability of production lines to different work tasks is also increasing, and the scenes where humans and robots cooperate to complete production tasks are gradually increasing. In order to improve the control accuracy and at the same time ensure the safety of human-computer interaction, a new type of manipulator system, the flexible manipulator system, is proposed. Flexible manipulators are divided into flexible link manipulators and flexible joint manipulators.

Based on random matrix and screw theory, this paper uses system decomposition technology to express the dynamic information of flexible manipulators in steady state and uses a random matrix network to construct a learning controller for the same or similar control tasks, avoiding repeated training. High-performance control is achieved. The controller estimates motor uncertainties, load disturbances, and joint friction in real time through the extended state observer (ESO) and compensates for various nonlinear factors during the control process. Simulation analysis shows that the designed double closed-loop ADRC controller can not only meet the requirements of the flexible joint system for rapidity and steady-state accuracy but also effectively suppress the influence of motor uncertainties, load disturbance, and friction on the system. The controller algorithm is simple and easy to implement digitally. Firstly, for the flexible joint manipulator system with unknown nonlinear dynamics, a random matrix network is used to approximate the unknown dynamics of the system, and combined with the dynamic surface control technology, a random matrix network controller is designed to solve the problem of dimension explosion and ensure the tracking error, and it converges to a small neighborhood of zero. Subsequently, in order to avoid using multiple random matrix networks to identify the unknown dynamics of the system and reduce the computational complexity of the control algorithm, a system conversion method was used to convert the flexible joint manipulator model with unknown dynamics into a canonical system. A high-gain observer is designed to observe the unmeasured part of the state of the converted system. Combined with a high-gain observer, a random matrix network controller is designed to realize the tracking control of the system. On this basis, using the random matrix function, only the dynamic information of a system needs to be expressed, stored, and reused, and the random matrix network learning controller is constructed to apply to the same or similar control tasks, avoiding the complex weight convergence verification process. Therefore, the study of neural network control and learning of flexible joint manipulators has important theoretical significance and broad practical application prospects.

2. Related Work

The robot arm is usually a multi-degree-of-freedom space open or closed chain mechanism connected by a series of links through a combination of rotating joints or moving joints (kinematic pairs). First of all, it is necessary to clarify the position coordinate relationship between these

moving links, then describe their relative motion relationship, establish the coordinate transformation relationship from the base coordinate to the end tool coordinate system to study the motion law of the robot, and realize the transformation from joint space to flute spaces [14–16].

The inversion method is used to solve the influence of nonmatching uncertainty on the control system. Combined with the random matrix network, an adaptive random matrix network control method is proposed to ensure system stability and trajectory tracking. Kuang and Zheng [17] proposed an underwater robot control method based on the inversion method and discussed the adaptive inversion manipulator control technology for the nonlinear model of uncertainty and external disturbance. Dai et al. [18] proposed a random matrix network inversion control method, which uses a random matrix network to approximate the system uncertainty and introduces a random matrix surface in the process of virtual control quantity design to improve the control performance. At the same time, in actual production, it is very common for robotic arms to perform the same or similar tasks repeatedly. How to save the knowledge of random matrix network identification system dynamics, realize the learning of system dynamics, and avoid repeated training of random matrix network is a research direction of great theoretical significance. And because of the limitations of sensor deployment and the influence of external interference, we often cannot obtain all the state variables of the system.

Firstly, the size optimization design was carried out using the software. Yang et al. [19] set the optimization goals as joint torque and operational performance parameters and used the shape and size parameters of the robot arm as design variables. In order to analyze the performance of different optimization algorithms, Molina used different optimization algorithms. The optimization algorithm compares the optimization of different boom section sizes and finally obtains the optimal rod section size parameters [20]. Shape and topology optimization is usually combined with CAE software such as ANSYS for mechanical structure optimization. Qiao et al. [21] studied and analyzed the time convergence characteristics of manipulator control, such as linear manipulator, terminal manipulator, and nonsingular terminal manipulator controller, and summed up the design experience of the above methods, and based on this, an appropriate index was designed in the manipulator surface. A new global fast nonsingular manipulator hypersurface is studied by using random matrix function and adjustment parameters, and the superiority of its convergence time characteristics is verified by comparative experiments. At the same time, we try to combine the fuzzy control strategy to adjust the switching gain of the manipulator control, so as to alleviate the chattering problem encountered in the controller design process and improve the overall performance of the controller. In the case of a certain unknown model error and external disturbance, a trajectory tracking test of the serial robot is designed to verify the robustness of the control algorithm and the fast error convergence characteristics [22–24].

3. Random Matrices and Spinor Theory Architecture

3.1. Random Matrix Space Equation. In any random matrix space segment, to make the random matrix function S continuously excited, its input vector Z must pass through the small neighborhood ε of all neuron centers within the minimum time interval. But in real systems, the trajectory may only pass through a small neighborhood of the center of some neurons, so this conclusion does not apply to most engineering practices. In order to make the continuous excitation condition of the random matrix network more widely used, the introduced random matrix function will relax this restriction.

$$s(i, j): \begin{cases} [i(1-a), i(a), \dots, i(1)] \\ [j(1-a), j(a), \dots, j(1)] \end{cases} \in R. \quad (1)$$

What is shown is the change of the eccentricity of the total trajectory control relative to the joint b of the manipulator in the fixed coordinate system of the case. A body can indirectly reflect the change in the attitude of the space station during the transposition process. In addition, by considering the eccentricity in the modeling process, the model that should be represented by a differential-algebraic equation can be transformed into a model represented by a random matrix function, which is beneficial to the calculation and analysis of the dynamic model. It is generally believed that an important way to improve the accuracy of the robot is the error compensation of geometric parameters, that is, parameter calibration.

On this basis, using the deterministic learning theory, it is only necessary to express, store, and reuse the dynamic information of a system and construct a neural network learning controller for the same or similar control tasks. The so-called calibration is to use advanced measurement methods and model-based parameter identification methods to identify the accurate parameters of the robot model. The process of controlling algorithms is given to compensate for robot errors, thereby improving the absolute accuracy of the robot.

$$\frac{a(i, j)}{1 - a(i)a(j)} < \int \frac{\partial \log(i-1)}{\partial \log(i-1)} di - \frac{1 - \partial \log(i-1)}{\partial \log(i)} di. \quad (2)$$

In this paper, when the trajectory control method is used to describe the elastic deformation of the flexible arm, the linear elastic mechanics category is mainly considered. Its basic characteristics are as follows: the equilibrium equation is a linear equation that does not depend on the deformation state; the relationship between the strain and displacement of the geometric equation is linear; the relationship between the stress and strain of the physical property equation is linear; the external force on the force boundary and the displacement boundary is linear. The displacement of it is independent or linearly dependent on the deformation state.

3.2. Boundary Conditions of Screw Theory. In order to carry out the modal analysis of the boundary random matrix in

screw theory, it is necessary to transform the physical coordinates in the linear random matrix function describing the flexible body into modal coordinates.

$$\begin{cases} \forall \frac{dx(s, t)}{dsdt} < \frac{x(s, t)}{x(s)x(t)}, \\ \exists t - x(t) > 0. \end{cases} \quad (3)$$

According to the random matrix modal analysis, the essence of the motion of the object can be revealed. By measuring the energy contribution of each order random matrix modal in the system response, the random matrix modal truncation criterion in Table 1 can be established, thereby reducing the number of equations.

In order to ensure that the control of the space flexible manipulator meets the requirements, the random matrix modal analysis is an important work in the research of manipulator dynamics. Because it is necessary to accurately grasp the vibration frequency of the manipulator in various configurations, a more accurate observer can be designed to estimate the random matrix modes of vibration (such as random matrix modal coordinates and random matrix modal velocity), which is more conducive to the design. The corresponding joint controller suppresses the random matrix mode of flexible vibration of the manipulator while realizing the rotation task. Taking the robot as an example, the dynamic model of the robot is derived by using the symbolic computing software, which is the basis for the subsequent motion control of the robot based on the dynamic model.

$$\begin{cases} M(x, y) \longrightarrow R(x, y - x), \\ m(x)m(y) \longrightarrow R(x - y, y). \end{cases} \quad (4)$$

The flexibility of the joint is caused by the reducer, the shaft, and the transmission gear, which can be approximated as a torsion spring. The influence of joint flexibility on the positioning of the manipulator is essentially similar to that of the link flexibility, and it can be equivalently considered that the random matrix modes of the flexible joints are superimposed. Therefore, the calculated value of the random matrix modal frequency in this paper will be higher than the actual value in the project, but this will not affect the convincing and correctness of the vibration control simulation results in the subsequent chapters.

3.3. Trajectory Control Detection. According to the relevant theory of trajectory control synthesis, the application of this method for vibration suppression requires accurate acquisition of the frequency and system damping coefficient of the random matrix mode to be suppressed. However, due to the limitations of modeling methods, system parameter perturbation, and possible errors in parameter identification in practical applications, it is difficult to obtain accurate parameters of system frequency and damping. Then, the observed value is used to replace the unmeasurable state of the system, combined with the RBF neural network to identify

TABLE 1: Boundary conditions of screw theory.

Boundary index	Object a	Object b	Object c	Object d	Object e	Object f
Truncation value	80.696	52.487	67.301	21.913	21.309	63.770
Mean value	0.121	0.993	0.322	0.006	0.086	0.412
Random value	0.004	0.553	0.346	0.807	0.525	0.673
Criterion value	0.219	0.213	0.638	0.484	0.437	0.429

the unknown dynamics of the system, and a neural network controller is designed to realize the tracking control of the system and ensure that the tracking error converges to a small neighborhood of zero.

$$\begin{bmatrix} \frac{a(i)-1}{a(i)} & -1 \\ 1 & \frac{a(i)-1}{a(i)} \end{bmatrix} = \begin{bmatrix} \frac{b(i)-1}{a(i)-b(i)} & -i \\ i & \frac{b(i)-1}{b(i)} \end{bmatrix}. \quad (5)$$

The existence of system parameter error will lead to the existence of residual vibration. It can be proved that the random matrix network weights can converge to a certain constant value. By saving this part of the constant network weights, the learned random matrix network can be stored, and the random matrix network can be directly called when encountering the same or similar tasks, avoiding the online adjustment process and saving computing resources.

In order to verify the influence of the trajectory control input signal in Figure 1 on the system, under the action of the conventional PD controller, different input signals are selected to carry out the position trajectory tracking experiment of the joint output end. PD controller parameter selection: $K = 40$, $t = 0.05$, when the input signal is a unit step signal, the position tracking and torque fluctuation of the system are shown in the text. In order to verify the influence of different input signals in the spring-damper model on the system, the conventional PD feedback control is still used, and different input signals are selected for the position trajectory tracking experiment of the joint output.

For the vast majority of periodic or periodic-like trajectories, neurons along the trajectory can satisfy the continuous excitation condition. This conclusion greatly relaxes the constraints on satisfying sustained incentives. The values of the controller parameters are the same as those in it, and the input signals are unit step signal, ramp signal, and sinusoidal signal, corresponding to the system position tracking curve and torque fluctuation curve in Table 2, respectively.

It can be seen from the complexity of the formula and the total amount of measurement that the calculation amount of the original Lagrange method is many times larger than that of the Newton-Eulerian method, while for the random matrix method, the calculation amount can reach $O(n=2)$. However, when the number of joints is small ($n < 4$), the amount of calculation is far less than that of other dynamic modeling methods, and with the random matrix equation combined with the screw theory, the modeling process geometry meaning is more obvious and easy to infer.

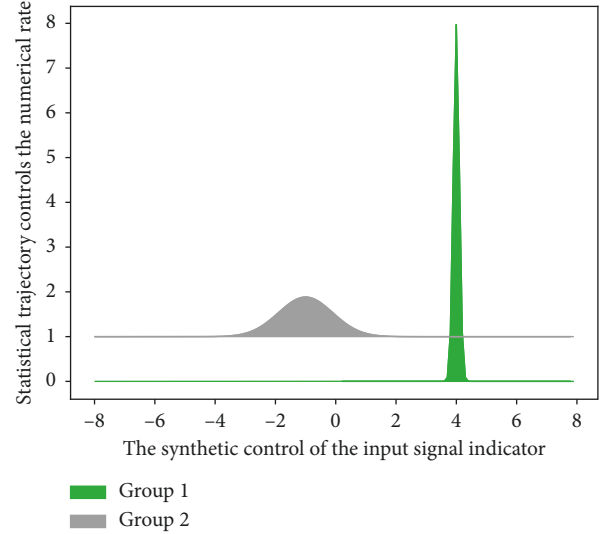


FIGURE 1: Trajectory control synthesis control input signal.

$$\text{erist}(x, \text{mean}(x, x-1)) = \begin{cases} \frac{1 - \text{mean}(x, x-1)}{\text{mean}(x, x-1)}, & x > 1, \\ x \left[x-1, \frac{\text{mean}(x, x-1)}{x} \right], & x < 1. \end{cases} \quad (6)$$

It can be seen that, considering the effectiveness of various dynamic algorithms, different modeling methods can be selected according to different modeling objects and the number of joints.

4. Construction of Trajectory Control Model of Flexible Joint Manipulator Based on Random Matrix and Screw Theory

4.1. *Random Matrix Exponential Analysis.* The random matrix exponential method is a new method developed to establish the dynamic equation of the multi-degree-of-freedom system. The motion of the system is described by independent variables, and the focus is on the motion, not on the configuration, which can avoid the cumbersome steps of using dynamic random matrix function derivation.

$$\begin{bmatrix} a(i, j) \\ b(i, j) \\ c(i, j) \end{bmatrix} \in \begin{bmatrix} R(i, j) \\ R(i-1, 1-j) \\ R(i+j) \end{bmatrix}. \quad (7)$$

TABLE 2: System position tracking trajectory algorithm.

System position test step	Tracking trajectory algorithm text
Import matplotlib.pyplot as plt	Method is many $x(t-1)$ times
Plt.rcParams ['font.sans-serif'] = ['simhei']	Larger than that of the $z(i)$
Plt.rcParams ['axes.unicode_minus'] = False	T can be seen $\sin(t)$
Fig = plt.figure ()	From the $z(i-1)$ complexity
Ax = fig.add_subplot (111, polar = True)	The original Lagrange
Ax.plot (angles, values, 'o-', lw = 2)	Of the formula and $\cos(a-b)$
Ax.fill (angles, values, alpha = 0.15)	The calculation amount of $u(a,b)$
Ax.set_thetagrids (angles * 180/np.pi, features)	The total amount germist (x)
Ax.set_ylim (0, 5)	Of measurement that $1 - \sin(t)$
Plt.title ('')	$z(y-x)(y+x)$

Pseudo-coordinates are linear combinations of derivatives of random matrices. In this way, pseudo-coordinates can be combined in many different ways. The problem can also be considered from various perspectives. In the process of dealing with different problems, the graph can be selected according to the specific situation. By saving this part of the constant network weights, the learned empirical knowledge can be stored, and the empirical knowledge can be directly invoked when encountering the same or similar tasks, avoiding the online adjustment process and saving computing resources.

It can be seen that the influence of different controller parameters on the spring-damper model is consistent with the simulation results of the linear torsion spring model in Figure 2. It can speed up the position tracking response speed and make the position curve approach the desired curve faster; reducing can increase the overshoot of the position tracking curve and at the same time reduce the intensity of torque oscillation.

$$\begin{bmatrix} \text{eper}(t) - t \\ \text{eper}(t-1) - t - 1 \\ \text{eper}(t+1) - t + 1 \end{bmatrix} = \text{deltar}\left(\frac{t}{-1-t, t-1}\right). \quad (8)$$

The random matrix leveling effect test is mainly to test the leveling effect of transverse and longitudinal slopes under different slopes and different loads. After the leveling control system is started and stabilized, the balance of the workbench is tested, and the inclination angle between the workbench and the horizontal plane is used as the adjustment leveling error. When the platform does not rise and fall, the inclination sensor measures the inclination angle of the worktable in real time and displays it on the touch screen. When the data fluctuates within a certain range, the engine stops running, and the inclination angle of the worktable is measured by the DMI108 digital display inclinometer.

4.2. Discussion on the Stability of Screw Theory. When the error of the theoretical parameters of the screw is large, the residual vibration may be very large, and the ideal vibration suppression effect cannot be achieved. First of all, the single-rod manipulator has the advantages of simple structure

design and control, high control precision, and easy ground test. Using it to realize cabin indexing is a simple, reliable, and cost-effective means. For the overall closed loop with the level of interference attenuation, unequal in a linear matrix in sufficient condition for its stochastic stability is given in the form of it.

$$\text{wister}(s, t) = \frac{1}{s-t} \int \frac{\partial \log(j-1)}{\log(j-1)} dj + \int \frac{\text{dine}(x-1)}{\text{ine}(x-1)} dj. \quad (9)$$

Secondly, considering that the operating motion of the two-rod flexible space manipulator can be completely decomposed like SRMS when the frequency is very low, it is not necessary to move at the same time, so it can be simplified for the study of the dynamics of the single-rod flexible manipulator. In addition to the above two points, the dynamics of a single-rod flexible manipulator are simpler than those of a two-rod flexible manipulator, but it is an important basis for understanding the complex dynamic properties of the flexible manipulator, and some of its important dynamic characteristics are given. The control of flexible robotic arms is also beneficial.

The position feedback of the space manipulator joint system generally includes two feedback forms, the motor position feedback and the position feedback of the joint output as shown in Figure 3. According to the different positions of the installation position feedback sensor, the control system can be further divided into a semiclosed-loop control system and a fully closed-loop control system. When the position feedback sensor is installed on the position of the motor shaft to indirectly measure the joint output position, it is called a semiclosed-loop system.

$$\text{herzer}(z, x, y) = \sum_{i=x,y,z} \overline{\text{eper}(i+1)} + \frac{1}{1 - \overline{\text{eper}(z+1)}} \quad (10)$$

It can be seen that under the action of the screw theory controller u , the actual output y of the system tracks the reference trajectory dy in a short period of time and is basically consistent with the reference trajectory after that, indicating that the tracking effect is fast and accurate, and the controller meets the basic control requirements. It can be seen that the state variables $2x$, $3x$, and $4x$ of the system state are all maintained in the interval $[-5, 5]$ after stabilization,

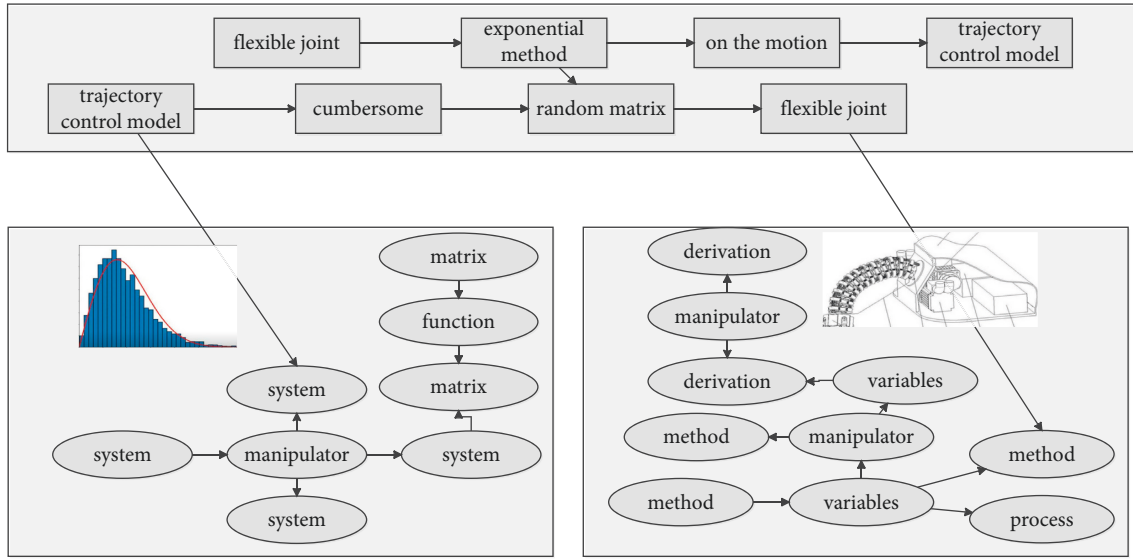


FIGURE 2: Random matrix exponential analysis topology.

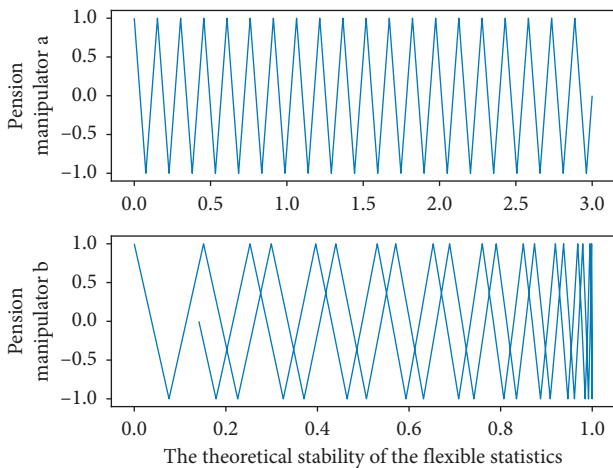


FIGURE 3: The theoretical stability of the flexible manipulator screw.

indicating that the state variables of the system are bounded. When constructing the sliding surface, a special set of matrices is established to associate each state observer and each sliding surface.

4.3. Flexible Joint Node Conversion. When the attitude angle or attitude angular velocity of the flexible joint reaches a certain limit, the manipulator is locked, and the attitude is controlled by the jet thrust. When the attitude of the space station returns to the initial position, the manipulator continues to index. The method adopted in the no-jet control strategy is to plan the inversion trajectory and the attitude of the space station during the inversion process and use the gravity gradient moment to unload the control moment gyro (CMG) angular momentum in real time to avoid CMG saturation.

$$\text{image}(\alpha, \beta) + mg \sin(a + b)\cos(a - b) + ka - b = 1. \quad (11)$$

When the nonjet attitude control strategy is unable to complete the on-orbit operation task and the actuator reaches saturation, the jet can be used to unload the angular momentum. Passive control mainly absorbs or consumes the vibration energy of flexible structures through vibration absorption, vibration isolation, energy consumption, and other means to achieve the purpose of suppressing vibration. And due to changes in subsystem connections, environmental interference, etc., the system structure may change abruptly; the data transmission and limited data processing capacity between the various components of the system will cause time delays; in addition, the system may contain uncertain factors.

When the nonlinear factors are not considered, the semiclosed-loop PD position control structure of flexible joints can track the given input trajectory well, while the full closed-loop PD position control effect is not as ideal as the semiclosed-loop PD position control. Figure 4 reflects the size of the trajectory tracking error. The steady-state error of the system under semiclosed-loop control remains at 0.86 Rad, and the steady-state error remains at 0.1 Rad. It can be seen that the semiclosed-loop control effect is better than the full closed-loop control when the nonlinear factors are not considered. When the nonlinear factors of the system are considered, the semiclosed-loop PD position control trajectory tracking effect is better than full closed-loop PD position control, and the changing trend tends to be unstable.

$$\begin{bmatrix} fn \cos(a - b)\sin(a + b) \\ mg \sin(a + b)\cos(a - b) \end{bmatrix} = \begin{bmatrix} v(a, b) \\ u(a, b) \end{bmatrix}. \quad (12)$$

First, the sliding surface is designed, the equivalent control is obtained through the sliding surface, and the sliding mode is further obtained. The system state is close to or has entered the quasi-sliding random matrix mode, the robustness of the system is gradually enhanced, the state error converges according to the specified state, the surface

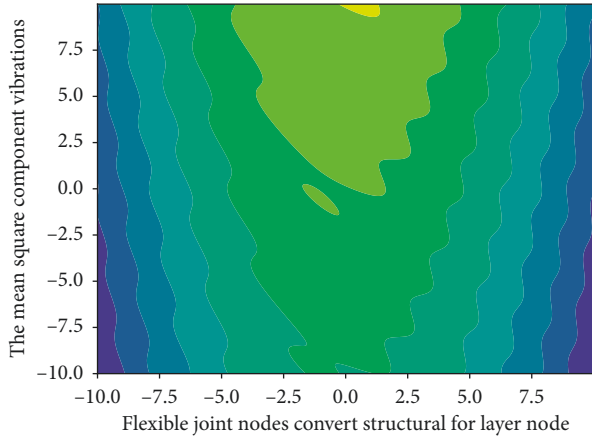


FIGURE 4: Flexible joint node transformation structure vibration.

variables of the manipulator are closer to the sliding random matrix mode, and the control output should be small at this time to prevent. The output torque of the controller is too large, which causes $s(f)$ to frequently cross the manipulator switching lines $(t)=0$ under the action of inertia, which stimulates chattering.

4.4. Robotic Arm Trajectory Control Design. The manipulator trajectory expansion state observer is the core component of the active disturbance rejection control technology. It is improved on the basis of the state observer. The observer only needs to use the input and output of the observed object as the input of the observer. By expanding the state observer, not only can the estimated value of each state variable of the observed object be obtained, but also the real-time action amount of the uncertain model and external disturbance can be estimated, and the uncertainty of the controlled object can be compensated by feedback, so as to achieve the reconstruction of the controlled object and simplify the design purpose of the control system.

$$\begin{cases} x(t) = f(x < t | x(t-1)), \\ y(t) = \frac{mg \sin(t)}{1 - \sin(t)} \sin(t) - (x(t) - t). \end{cases} \quad (13)$$

When the conventional PD position controller is simply used, the joint torque changes drastically, and the jitter of the joint is large; when the PD position control with negative torque feedback is used, the change of the joint torque is significantly reduced, and the jitter of the joint is greatly reduced. For the sliding mode system, a Lyapunov function is constructed and the function is processed to obtain the sufficient condition for the random stability of the sliding mode, which is given in the form of linear matrix inequality.

It can be seen that the tracking error experienced some relatively large fluctuations in the time shown in Figure 5, stabilized after the 20th second, and maintained a relatively small fluctuation near zero. Although there is always a certain tracking error, the value of the error is very small and within an acceptable range, which indicates that the

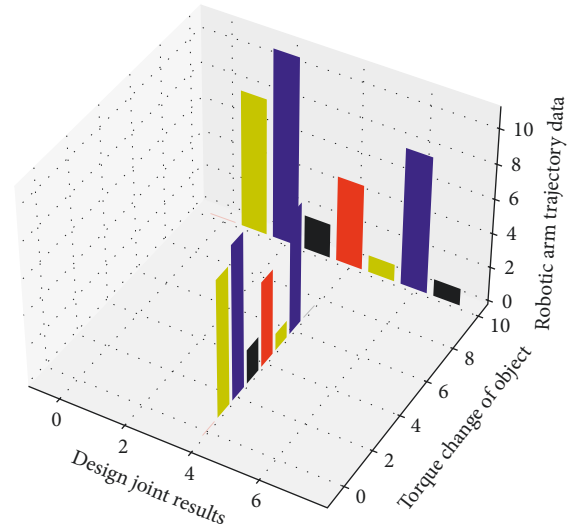


FIGURE 5: Changes in joint torque of the robot arm trajectory control design.

designed controller has good tracking performance. At the same time, in order to verify the application effect of the designed controller algorithm in the actual system, we also conduct experiments on the Baxter robot platform. The joints of the Baxter manipulator are flexible and conform to the model of the control algorithm we designed.

$$\begin{cases} z(y)z(x) = z(y-x)(y+x), \\ z(y-x) = \text{germist}(y) - \text{germist}(x) + \frac{k}{(x-y)}. \end{cases} \quad (14)$$

Judging by the attitude maneuver time index, under various obstacle avoidance conditions, the GPM index is the best, followed by the Bezier random matrix function method, and the FFS random matrix function method requires the longest maneuvering time. In this case, the performance improvement of the optimal solution of maneuver time obtained by the above three methods is only 3.22%, 3.50%, and 3.43% compared with the worst solution. When the calculation time of trajectory generation is used as the judgment index, it is obvious that the method using the random matrix function has better performance than GPM.

5. Application and Analysis of Trajectory Control Model of Flexible Joint Manipulator Based on Random Matrix and Screw Theory

5.1. Random Matrix Solution Set Preprocessing. Considering that the system has rigid body motion vibration and flexible random matrix modal vibration, the random matrix mode of rigid body motion and the first-order flexible system random matrix mode are suppressed, and the random matrix solution set cascade method is used to design. Firstly, the corresponding flexible manipulator S_r is designed for the vibration random matrix mode of rigid body motion, and then the corresponding flexible manipulator S_f is designed

for the flexible random matrix modal vibration. Finally, the obtained flexible manipulators are cascaded and combined into a new flexible manipulator to achieve simultaneous vibration suppression of rigid body motion vibration and flexible random matrix modal vibration.

$$\sum_{i=1}^{i+k-1} z(i) \cup z(i-1) \subseteq \sum_{i=1}^{i+k-1} \frac{z(i, j)}{z(i)} \cup \frac{z(i-1)}{z(j) - z(i, j)}. \quad (15)$$

It can be seen that the three schemes can effectively complete the 60° maneuvering task of the flexible manipulator, and the rise time used is about 13.5 s, 14.9 s, and 14.3 s, respectively. Scheme (1) makes the first-order random matrix modal coordinates of the manipulator continue to vibrate for a long time, and the elastic deformation of the end is also large. Both scheme (2) and scheme (3) can quickly suppress the vibration of the flexible manipulator. The application of the pulsed MUM flexible manipulator in Figure 6 improves the system rise time by 0.6s compared with the application of the UM-ZVD flexible manipulator. The simulation results show the effectiveness of the proposed method. Then, the controller is designed to ensure that the sliding surface is reachable. At the end of the chapter, a numerical example is used to illustrate the validity of the conclusions.

With the increase of the torque negative feedback coefficient t , the vibration amplitude of the joint moment of the random matrix solution set becomes smaller, the amplitude of the residual vibration becomes smaller and smaller, and the vibration suppression effect of the joint is better. After the sliding mode surface design, the next important task is the design of the sliding mode controller. Now, we design a sliding mode control law to ensure that the closed-loop system can reach the sliding mode surface in a finite time.

5.2. Simulation of Trajectory Control of Flexible Joint Manipulator. The interference signal here is Gaussian white noise signal. The parameters of the filtering algorithm are $A = 0.5$, the position control gain $K_p = 40$, the speed control gain 0.05, and torque negative feedback gain coefficient $A/q = 10$, such as $f = 0.5$. The simulation experiments are carried out using torque negative feedback control and torque negative feedback PD control, respectively. The Baxter robot operation platform we use is composed of the Baxter robot and the control host console. The Baxter robot has a total of 7 flexible joints. It can be seen that the output of the control algorithm in Figure 7 applied to the Baxter robot experimental platform is relatively close to the previous MATLAB simulation results, in which the system output on the Baxter platform has a small delay, which is related to the physical inertia of the robotic arm system.

The response time and leveling effect test of the leveling system of the flexible joint manipulator were carried out. The response time of the leveling control system includes the computing time of the single-chip microcomputer, the signal acquisition time of the inclination sensor, and the action response time of the solenoid valve and the leveling cylinder. Since the operation and signal acquisition of the

single-chip microcomputer are completed in the system scan cycle, it can be ignored.

First, the corresponding sliding mode surface is designed for each system, and then a sliding mode control rate is used to ensure the accessibility of the sliding mode surface; then, the corresponding equivalent control is designed to ensure the stability of the sliding mode. The platform is on a horizontal hard surface, and the beam rotates at a constant angular speed. Within 0.03 degrees, it is about the comparison algorithm, even in the initial state of joint 3, the maximum error is 0. Within 0.2 degrees, and without accumulating errors in the initial stage, the nonlinear integral term eliminates steady-state errors well.

Figure 8 shows the identification effect of the random matrix network on the unknown dynamic $H(x)$ of the system. The simulation results show that the random matrix network can effectively approximate the unknown dynamic of the system. And it can be seen that the weights of the random matrix network converge after 300 seconds, so we average the weights of the neural network in the [400,500] second interval and save them as the stored random matrix network. Next, we use the stored empirical knowledge to construct a random matrix network WSX with constant weights to fit the unknown nonlinearity $H(x)$ of the system and design a learning controller. A comparison of the tracking errors in the learning phase and the training phase is given. The simulation results show that although the initial error in the learning phase is set to be relatively large, it can still converge faster than the training phase, and after convergence, the steady-state error in the learning phase is also less than it. The steady-state error in the training phase shows that the system can track the upper reference trajectory faster, and the transient and steady-state properties of the system have been effectively improved.

5.3. Example Application and Analysis. The membership random matrix function of the design input variables of the flexible joint manipulator is eccentrically distributed. The lower the language value level is, the narrower the membership random matrix function covers. Such a design can enhance the sensitivity of the controller to the input when the manipulator surface variables and errors are small, improve the system resolution, and reduce the controlled parameters to a sufficiently small size before the manipulator surface variables reach the boundary layer to prevent chattering. However, when the surface variables and errors of the manipulator are large, the output parameters of the controller change slowly, so as to keep the surface variables of the manipulator with sufficient convergence speed and ensure the rapidity of the system. Both comparison algorithms can finally reach the manipulator surface, and both can converge to the equilibrium point in a limited time.

When analyzing the stability of the corresponding sliding mode system, different Lyapunov functions are constructed and derived, and then, the derivation results are processed by using the corresponding lemma, and finally, the linear matrix inequality sufficient condition for the

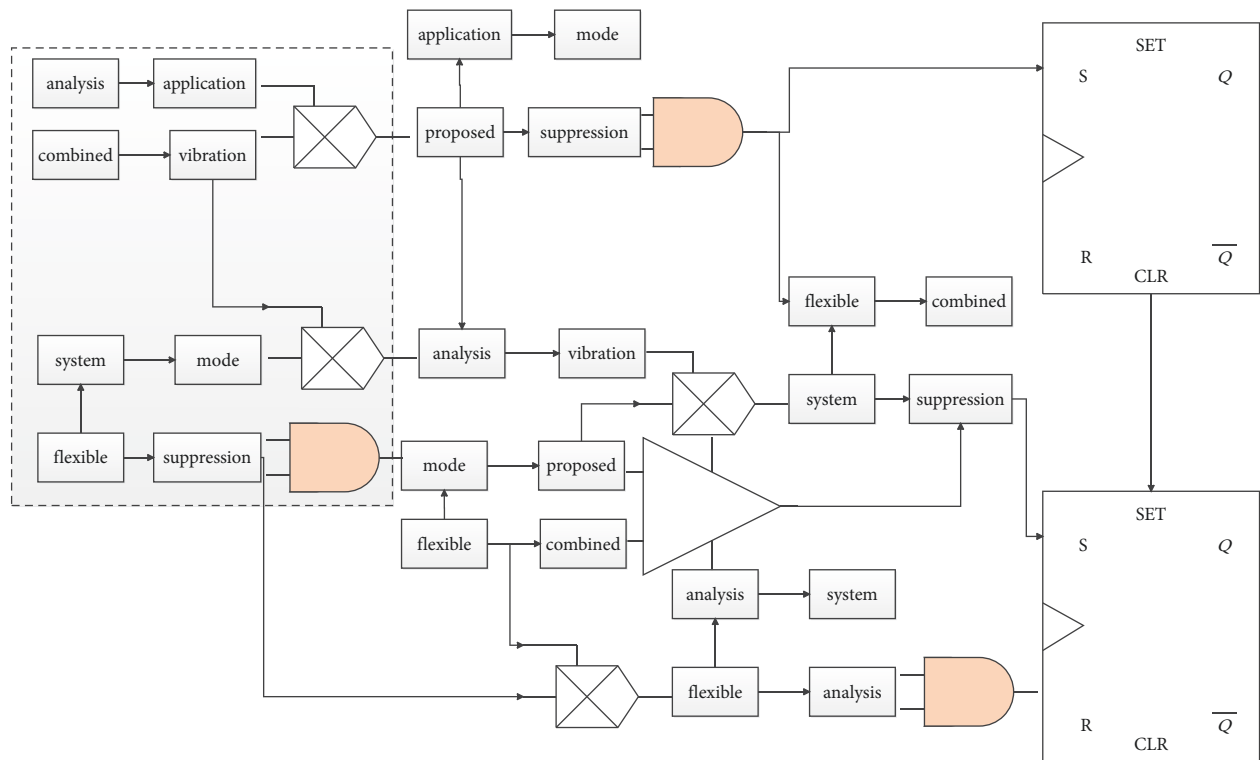


FIGURE 6: Preprocessing analysis of random matrix solution set.

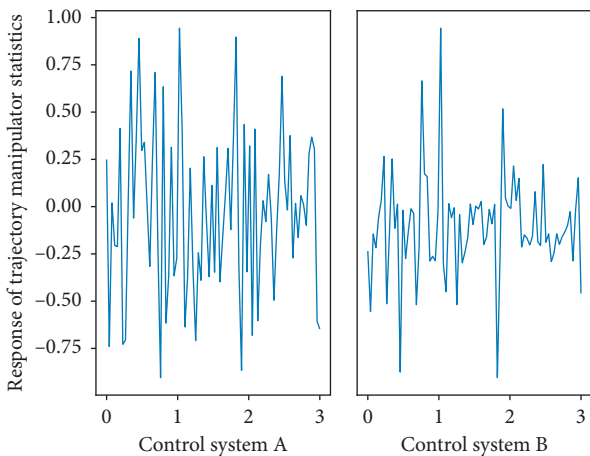


FIGURE 7: Response of trajectory control system of the flexible joint manipulator.

stability of the sliding mode is given in the form. Approaching the equilibrium point of the system, when the systematic error of Figure 9 is small at 1.5 s to 2 s, the convergence rates of the two are equivalent.

In order to ensure that the manipulator can be realized within the expected time and maintain good dynamic quality, the approach law method is used to design the manipulator controller for robot trajectory tracking. It reaches the surface of the manipulator within time and then realizes the motion of the manipulator, and different reaching laws determine that the dynamic characteristics of the system state entering the sliding mode surface are

different, and the degree of chattering will be different. In this chapter, the exponential approach law is selected, and the approach speed is gradually reduced from a large value to zero, which not only shortens the approach time but also makes the speed of the moving point to the switching surface very small, resulting in less chattering and approach. The speed is fast and the amount of calculation is moderate so that the system has a controllable and better dynamic process. In the case of some unobtainable state quantities in the system itself, a neural network state observer is designed to observe, which solves the problem that part of the state cannot be obtained.

In the presence of noise interference, the PD control of torque negative feedback in Figure 10 can well achieve the filtering of noise signals and the impact of interference on the system. The vibration amplitude of the joints is relatively large, but in comparison, the torque negative feedback PD control has a smaller vibration amplitude. After 0.4 s, the anti-interference ability of torque negative feedback control is poor, the system is affected by the interference signal, the torque jitters violently, and the jitter frequency is high, while the torque negative feedback PD controls the joint torque to change less violently and the joint jitter amplitude is low with strong anti-interference ability. If the generalized system in question is slightly more complex, it is likely to make the results too conservative. It is easier to get better results if there is some better improvement in the solution of matrix inequalities, such as not being restricted to strictly linear or linear. It can be seen that after using the saturated random matrix function, the oscillation degree of the two joints is reduced by more than 50% compared with the sign

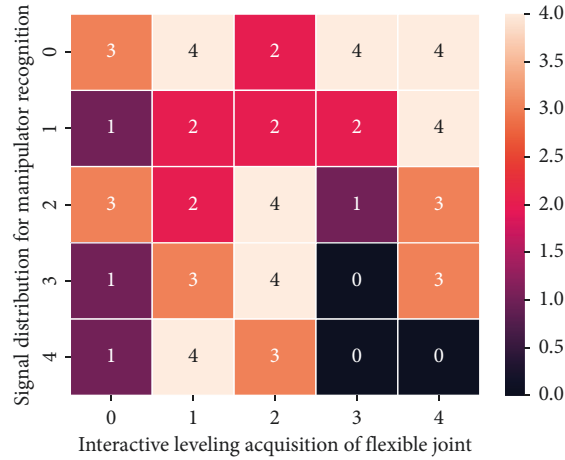


FIGURE 8: Signal distribution of leveling acquisition of flexible joint manipulator.

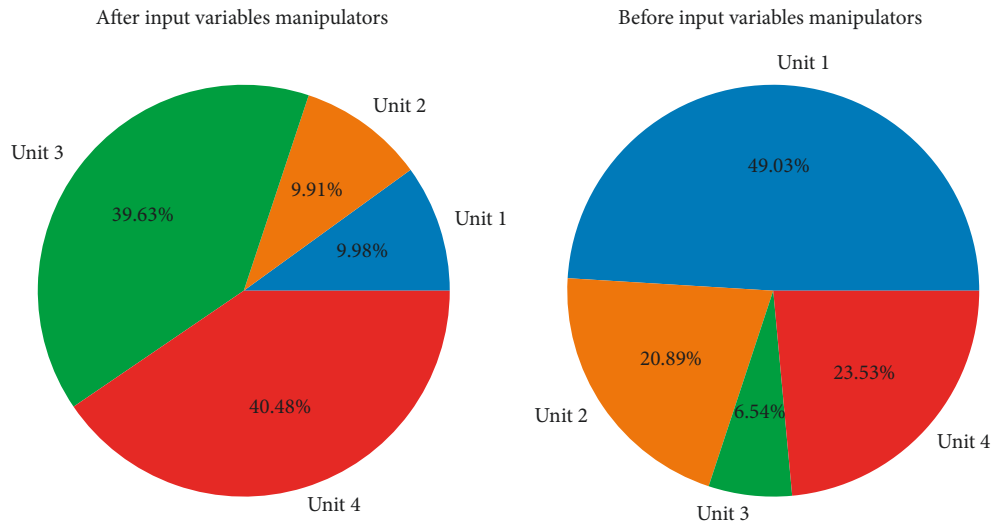


FIGURE 9: Distribution of input variables in the design of flexible joint manipulators.

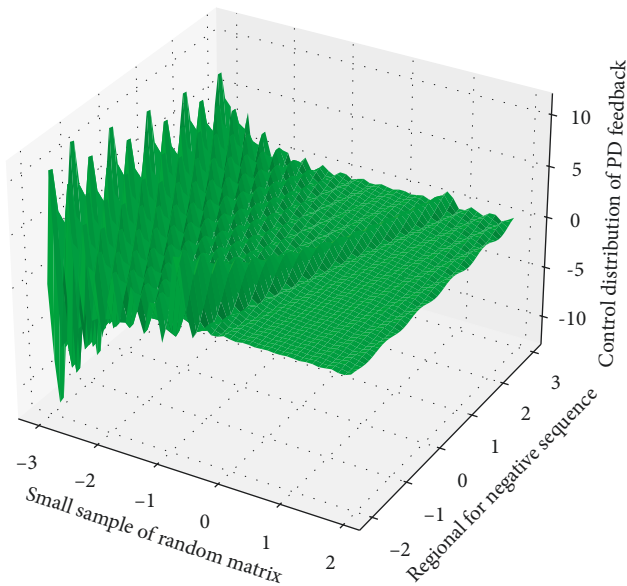


FIGURE 10: PD control distribution of random matrix torque negative feedback.

switching random matrix function, and the high-frequency fluctuation is small, which makes the controller output smoother and softer, which is beneficial to the protection of physical devices. It is also a very important factor in the practical application of manipulator control, but although the symbolic random matrix function is replaced in this chapter, the uncertainty of the system, including modeling errors and interference, needs to be estimated and set manually in advance, and the estimation is too large. It will cause unnecessary chattering and affect the control accuracy of the system. If the estimation is too small, it will affect the robustness of the system. Therefore, in the next chapters, this paper will continue to introduce a more flexible following estimation method to reduce the impact of chattering.

6. Conclusion

Aiming at the problem of high-precision trajectory tracking of flexible joints of space manipulators, this paper adopts a random matrix model, and according to different nonlinear factors, two types of flexible joint second-order linked

dynamic equations considering uncertain disturbance and both friction and uncertain disturbance are established, respectively. The two types of models are unified into the form of two series subsystems, and the series system composed of two series subsystems is further expanded into a new cascade linear system by using the extended state observer. The cascade system is based on the active disturbance rejection. In order to reduce the number of neural networks and transform the system, a high-gain observer is designed to observe the state variables that cannot be obtained in the transformed system. The control (ADRC) technique designs a double closed-loop control system including two active disturbance rejection controllers. Considering the difference and connection between component force synthesis and input shaping active vibration control method, this method designs the pulse sequence of the flexible manipulator to include multiple pulses with alternating positive and negative sequences, which are formed by the selected number of pulses and the system vibration frequency and damping ratio to directly determine pulse duration and amplitude. According to this method, an improved unit-amplitude input flexible manipulator and an improved negative input flexible manipulator are proposed for the undamped system and the damped system, respectively. The designed improved negative flexible manipulator is compared with the corresponding positive flexible manipulator. Compared with the corresponding negatively flexible manipulator, its main advantage is that there is no need to optimize the constraints and no complicated calculations, which makes the design of the flexible manipulator very simple.

Data Availability

The data used to support the findings of this study are available from the corresponding author upon request.

Conflicts of Interest

The authors declare that they have no conflicts of interest.

Acknowledgments

This work was supported by Design and Research on 7DOF Redundant Manipulator of Picking Robot (qjhz [2020] No. 128).

References

- [1] Z. Liu, J. Xu, Q. Cheng, and Y. Y. C. Zhao, "Trajectory planning with minimum synthesis error for industrial robots using screw theory," *International Journal of Precision Engineering and Manufacturing*, vol. 19, no. 2, pp. 183–193, 2018.
- [2] Z. Du, G. Y. Ouyang, J. Xue, and Y. B. Yao, "A review on kinematic, workspace, trajectory planning and path planning of hyper-redundant manipulators," in *Proceedings of the Electrical and Electronics Engineers International on Cyber Technology in Automation, Control, and Intelligent Systems (CYBER)*, pp. 444–449, IEEE, Xi'an, China, October 2020.
- [3] F. J. Torres, J. P. Ramirez-Paredes, M. A. Garcia-Murillo, and I. G. V. A. Martinez-Ramirez, "A tracking control of a flexible-robot including the dynamics of the induction motor as actuator," *IEEE Access*, vol. 9, pp. 82373–82379, 2021.
- [4] X. Zheng and G. Wu, "Kinodynamic planning with reachability prediction for PTL maintenance robot," *Proceedings of the Institution of Mechanical Engineers - Part I: Journal of Systems & Control Engineering*, vol. 235, no. 8, pp. 1417–1432, 2021.
- [5] F. Liu, H. Huang, B. Li, and Y. H. Hu, "Design and analysis of a cable-driven rigid-flexible coupling parallel mechanism with variable stiffness," *Mechanism and Machine Theory*, vol. 153, Article ID 104030, 2020.
- [6] Z. Wang, Z. Chen, C. Mao, and X. Zhang, "An ANN-based precision compensation method for industrial manipulators via optimization of point selection," *Mathematical Problems in Engineering*, vol. 2, p. 32, 2020.
- [7] F. Guo, G. Cheng, and Y. Pang, "Explicit dynamic modeling with joint friction and coupling analysis of a 5-DOF hybrid polishing robot," *Mechanism and Machine Theory*, vol. 167, Article ID 104509, 2022.
- [8] J. E. Lavín-delgado, S. Chávez-vázquez, J. F. Gómez-aguilar, G. Delgado-Reyes, and M. A. Ruiz-jaimas, "Fractional-order passivity-based adaptive controller for a robot manipulator type s," *Fractals*, vol. 28, no. 8, Article ID 2040008, 2020.
- [9] B. Rong, X. Rui, L. Tao, and G. Wang, "Theoretical modeling and numerical solution methods for flexible multibody system dynamics," *Nonlinear Dynamics*, vol. 98, no. 2, pp. 1519–1553, 2019.
- [10] L. Jia, Y. Huang, T. Chen, and Y. Y. J. Guo, "Mda + rrt: a general approach for resolving the problem of angle constraint for hyper-redundant manipulator," *Expert Systems with Applications*, vol. 193, Article ID 116379, 2022.
- [11] A. Beiranvand, A. Kalhor, and M. Tale Masouleh, "Modeling, identification and minimum length integral sliding mode control of a 3-DOF cartesian parallel robot by considering virtual flexible links," *Mechanism and Machine Theory*, vol. 157, Article ID 104183, 2021.
- [12] X. Chen, Q. Zhang, and Y. Sun, "Model-based compensation and pareto-optimal trajectory modification method for robotic applications," *International Journal of Precision Engineering and Manufacturing*, vol. 20, no. 7, pp. 1127–1137, 2019.
- [13] T. Long, E. Li, Y. Hu, and L. J. Z. R. Yang, "A vibration control method for hybrid-structured flexible manipulator based on sliding mode control and reinforcement learning," *IEEE Transactions on Neural Networks and Learning Systems*, vol. 32, no. 2, pp. 841–852, 2021.
- [14] G. Singh and V. K. Banga, "Combinations of novel hybrid optimization algorithms-based trajectory planning analysis for an industrial robotic manipulator," *Journal of Field Robotics*, vol. 2, pp. 24–26, 2022.
- [15] X. Wang, X. Liu, L. Chen, and H. Hu, "Deep-learning damped least squares method for inverse kinematics of redundant robots," *Measurement*, vol. 171, Article ID 108821, 2021.
- [16] C. Gang, G. U. O. Wen, J. I. A. Qingxuan, W. A. N. G. Xuan, and F. U. Yingzhuo, "Failure treatment strategy and fault-tolerant path planning of a space manipulator with free-swinging joint failure," *Chinese Journal of Aeronautics*, vol. 31, no. 12, pp. 2290–2305, 2018.
- [17] C. Kuang and X. Zheng, "Space trajectory planning of electric robot based on unscented kalman filter," *Jordan Journal of Mechanical & Industrial Engineering*, vol. 15, no. 1, 2021.
- [18] Y. Dai, C. Xiang, W. Qu, and Q. Zhang, "A review of end-effector research based on compliance control," *Machines*, vol. 10, no. 2, p. 100, 2022.
- [19] C. Yang, R. Kang, D. T. Branson, and L. J. S. Chen, "Kinematics and statics of eccentric soft bending actuators with

- external payloads,” *Mechanism and Machine Theory*, vol. 139, pp. 526–541, 2019.
- [20] F. A. Lara-Molina and D. Dumur, “Robust multi-objective optimization of parallel manipulators,” *Meccanica*, vol. 56, no. 11, pp. 2843–2860, 2021.
- [21] J. Qiao, H. Wu, and X. Yu, “High-precision attitude tracking control of space manipulator system under multiple disturbances,” *IEEE Transactions on Systems, Man, and Cybernetics: Systems*, vol. 51, no. 7, pp. 4274–4284, 2021.
- [22] Z. Zhan, X. Zhang, H. Zhang, and G. Chen, “Unified motion reliability analysis and comparison study of planar parallel manipulators with interval joint clearance variables,” *Mechanism and Machine Theory*, vol. 138, pp. 58–75, 2019.
- [23] M. Affan, S. U. Ahmed, and R. Uddin, “Pick-and-Place task using wheeled mobile manipulator-A control design perspective,” in *Proceedings of the Computing and Information Technology (ICCIT-1441)*, pp. 34–39, IEEE, Tabuk, Saudi Arabia, September 2020.
- [24] J. L. Pulloquina, V. Mata, Á. Valera, P. Zamora-Ortiz, and M. I. Díaz-Rodríguez, “Experimental analysis of Type II singularities and assembly change points in a 3UPS+RPU parallel robot,” *Mechanism and Machine Theory*, vol. 158, Article ID 104242, 2021.